

# APPLICABILITY OF BALL PENETRATION TEST IN THE NAKDONG RIVER DELTA

DUNG N.T.<sup>1</sup>, CHUNGS.G.<sup>2</sup>, HONGY.P.<sup>3</sup>, KWEONH.J.<sup>4</sup>

<sup>1</sup>Lecturer, Dept of Civil Engineering, Dong-A University, Busan, Korea

<sup>2</sup>Professor, Dept of Civil Engineering, Dong-A University, Busan, Korea

<sup>3</sup>Postgraduate student, Dept of Civil Engineering, Dong-A University, Busan, Korea

<sup>4</sup>Researcher, National Research Laboratory for Soft Ground, Dong-A University, Busan, Korea

**ABSTRACT:** Ball penetration test (BPT), in association with different field tests such as CPTU, field vane test (FVT), seismic dilatometer test (SDMT), was carried out at an investigation site in the Nakdong River delta, Busan, S. Korea. The main objectives of the BPT were to evaluate the ball factor (thus the undrained shear strength,  $S_u$ ) and sensitivity of the soft clay at the site. As the BPT was first applied to the delta, four different ball sizes were used to examine the behavior of the test compared with the conventional CPTU. It was found from the study that ball factors, unlike the cone factors, are independent on rigidity index ( $I_r$ ). The ball factors obtained from different ball sizes are quite similar to each other and slightly smaller than those obtained from theoretical solutions. The sensitivity of the test soil was found smaller than the ratio of initial penetration resistance to the remolded penetration resistance ( $q_{ball,ini}/q_{ball,rem}$ ). However, no clear correlation was obtained for the test soil.

**Keywords:** Soft clay, field test, undrained shear strength, sensitivity, CPTU, BPT, SDMT and FVT

## INTRODUCTION

The cone penetration test with pore water pressure measurement (CPTU) has been widely used as the primary tool in site investigation. The main advantages of the CPTU are that it provides reliable and continuous profiles of data of the soil with depth. Testing procedures and methods of interpreting the data of the CPTU have been discussed extensively in the literature (e.g., Lunne et al. 1997; Mayne, 2007).

One of the most common parameters derived from the CPTU is the undrained shear strength. The value can be calculated by using several forms (Lunne et al. 1997), however the most common form is given in Eq. (1). It is known that, the shear strength value depends very much on the corrected cone resistance ( $q_{cone,t}$ ), the in-situ overburden pressure ( $\sigma_{v0}$ ) and the calibrated cone factor ( $N_{kt}$ ). Especially in soft to very soft clays, the accuracy of  $q_{cone,t}$  value becomes less than that of medium to stiff clays or in sands (Lunne et al. 1997). In addition, estimating precise values of  $\sigma_{v0}$  and  $N_{kt}$  is often costly in both terms of time and finance. Recently, the accuracy of the CPTU data in soft clay has greatly been concerned rather than the capacity of the CPTU equipments. According to the International Reference Test Procedure (IRTP) (ISSMGE, 1999) soft clays (classified as class 1) are subjected to very

strict requirements of accuracy.

Another popular and effective tool to evaluate the undrained shear strength of clays is the field vane test (FVT). The main advantage of the FVT is that its field result can be used without calibrating with laboratory test data, although the correction for measured data is often required. However, the FVT also exposes several restrictions as the test can only provide discontinuous soil profile and is quite time-consuming job. The undrained shear strength obtained from the FVT is rather sensitive to the testing procedures, in particular the delay between inserting the vane and rotating it and the rotation rate.

Due to the aforementioned restrictions of the CPTU and FVT in soft to very soft clays, other full-flow penetrometers such as T-bar, ball penetrometers were introduced some years ago (Stewart and Randolph, 1991, 1994; Vallejo, 1982), but appear to have been taken up again recently (Randolph, 2000). The advantages of full-flow penetrometers relative to the conventional cone penetrometer include (Randolph, 2004): (i) the measured penetration resistance requires minimal correction for overburden pressure to obtain net resistance, by contrast with significant correction to the measured cone resistance; (ii) improved accuracy is obtained in soft soils due to the larger projected area; the higher penetration force improves

resolution and also reduces sensitivity to any load cell drift; (iii) closely bracketed plasticity solutions are available for obtaining undrained shear strength of clays; (iv) remolded shear strength (thus the sensitivity) can be assessed from cyclic penetrations and extractions of the full-flow penetrometers.

The ball penetration test was initially proposed for determining the penetration resistance of soft clays under deep waters (Randolph, 2000) where the large pore water pressure can greatly influence the estimated undrained shear strength. Recently, the BPT has also been used in investigation of soft marine clays and dragged soils in Japan (Nakamura et al. 2009). The BPT has also been used for characterization of peat (Boylan and Long, 2007). Comparative studies between the BPT and other penetration tests (e.g., T-bar penetration test, plate penetration test, CPTU) has been extensively carried out by group researchers headed by the Center for Offshore Foundation Systems, the University of Western Australia (e.g., Randolph, 2004; Chung and Randolph, 2004; Einav and Randolph, 2004; Low et al. 2008, Low, 2009, Zhou and Randolph, 2009). Most recently, a comprehensive study on remolded shear strength and sensitivity of soft clays using full-flow penetrometers has been reported by Yafate et al. (2009).

This paper focuses on the application of the ball penetration test (BPT) to soft clay at an investigation site in the Nakdong River deltaic area. The main objectives of the BPT herein are: (i) to compare penetration resistances obtained from different ball and cone sizes; (ii) to evaluate the ball factor ( $N_{ball}$ ) and remolded ball factor ( $N_{ball,rem}$ ); (iii) to find a possible correlation between the sensitivity and resistance ratio of initial penetration resistance to the remolded penetration resistance. To calibrate results obtained from the BPT, the CPTU with two probe sizes and FVT were also carried out at the same site.

## SITE DESCRIPTION

The test site (named as DIS-5) is situated in the floodplain (i.e., marginal basin) of the Nakdong River delta, which lies west of Busan City and its vicinities. More information about the test location can be found from Chung et al. (2010).

Figure 1 shows a geotechnical profile at the study site. The soil profile is covered by a surface layer of around 5m silty clay intercalated with some shell fragments, following by a rather uniform soft to medium clay layer which lies on very dense sand and gravel layer from 31m to 32m downward. It is noted that there is a dense shell

intercalated sub-layer from the depths of 19 to 23 m which the thickness varies significantly at the site as later shown in the ball resistance profiles. Geotechnical properties of the clay layer can be briefly described as follows: Bulk density ( $\gamma$ ) varies from 1.5 to 1.7 t/m<sup>3</sup>, and water content ( $w_n$ ) varies from 40% to 80%. The specific gravity ( $G_s$ ) is between 2.69 and 2.72, and plasticity index ( $I_p$ ) is between 20% and 40%. The undrained shear strength values ( $S_u$ ) at the site are from 15 kPa to 52 kPa varying rather linearly with depth (except values in the dense shell intercalated sub-layer).

## FIELD TEST PROGRAM

The BPT was part of the soil investigation program at the site. Besides the BPT, other field tests such as CPTU, Dilatometer test (DMT), Seismic dilatometer test (SDMT), Field vane test (FVT), and sampling for laboratory tests were also carried out. This section briefly describes the relevant tests used for this paper. Figure 2 shows the plan view of the field test locations which formed an approximate square net of 2 to 3m.

### Ball penetration test (BPT)

The BPT was carried out by using a 20-ton capacity CPT machine (the inset in Figure 4) which is able to conduct the CPTU in dense to very dense sands. The testing procedures were very similar to that of the CPTU except that the balls were used instead of the cone tip. To evaluate the variation of the ball factors with respect to ball sizes, four different ball sizes were used as illustrated in Figure 3. The balls Type-1 to Type-3 were made of duralumin while the smallest size was additionally made of copper. Figure 4 shows a step of the BPT at the moment just before the ball Type-2 was carried out. Table 1 shows basic parameters of the balls. In this study, the balls were made to associate with the cone of 15 cm<sup>2</sup>, thus the ball connector diameters were all the same of 4.37 cm. The projected area is the cross-sectional area of the ball corresponding to the maximum diameter, and the projected area ratio is the ratio of the cone cross-sectional area to the ball projected area.

The BPT was carried out at a constant speed of 20 mm/second which was the same speed applied to the cone penetration test (CPTU) at the site. For each ball type, cyclic test (penetrations and extractions) of 8 cycles was carried out at several depths to evaluate the remolded penetration resistance and consequently the sensitivity of the clay. The cyclic length of 1.0 m was applied for all test points.

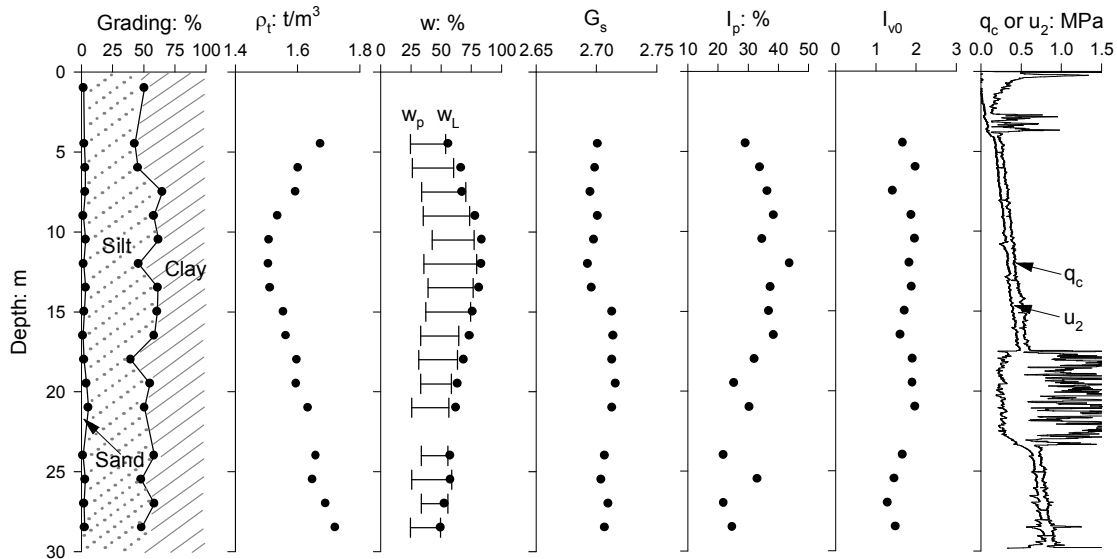


Figure 1 Geotechnical properties at the test site (Chung and Kweon 2010)

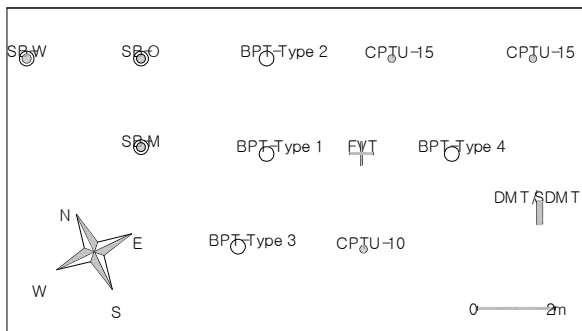


Figure 2 Plan view of the test locations



Figure 3 Ball types used for the tests

Table 1 Dimensions of different balls

Parameter	Type 1	Type 2	Type 3	Type 4
Diameter (cm)	11.28	8.74	6.18	4.37
Projected area (cm <sup>2</sup> )	100	60	30	15
Area of rod (cm <sup>2</sup> )	15	15	15	15
Projected area ratio	0.15	0.25	0.5	1.0

### Cone penetration test (CPTU)

The CPTU was performed at the site by using the same CPT machine. The test was performed at three locations

in which one was performed by using the cone of 10 cm<sup>2</sup> and the others by the cone of 15 cm<sup>2</sup> (denoted as CPTU-10 and CPTU-15 respectively in Figure 2). Both the cone types were electrical ones of 60° apex with a porous element (filter) mounted immediately behind the cone shoulder to measure induced pore water pressure ( $u_2$ ). Average penetration rate for the CPTU was also 20 mm/second.

### Filed vane test (FVT)

To calibrate the cone and ball factors at the site, the FVT was carried at the center of the CPTUs and BPTs as shown in Figure 2. The system used was Geonor type (H-10) with blade dimensions of 55 mm ( $B$ ) × 100 mm ( $H$ ). In this case, the field vane head was advanced directly (without pre-borehole) into the ground and stopped at 50 cm above the test depth. The blade connected to the inner rod was then pushed down to the test depth. After waiting 5 minutes, the test was carried out at a constant speed of 0.1°/second until the residual resistance became constant. The remolded test was also conducted at every test depths.

### Dilatometer and Seismic dilatometer tests (DMT/SDMT)

The DMT in association with SDMT (Marchetti's equipments) was also carried out at the site by using the same CPT machine as pushing system. The DMT blade was attached to a dual sensor system (50 cm in distance) which was then normally connected to CPT rods. The DMT and SDMT were alternately carried out at every 0.25 m intervals so that the SDMT-based and DMT-based parameters can be interpreted at every 0.5 m. A hard wooden block of 10 cm ( $H$ ) × 20 cm ( $W$ ) × 100 cm ( $L$ ) was

used as the plate to transmit seismic waves to the sensors and it was placed parallel to the chain of the CPT machine at a distance of 1.5m from the central rods.



Figure 4 Performance of the BPT at the test site

## DEFINITION OF PARAMETERS

### Net cone resistance and cone factor

In clays, an estimate of undrained shear strength from CPTU data is commonly expressed as:

$$S_u = \frac{q_{cone,net}}{N_{kt}} = \frac{q_{cone,t} - \sigma_{v0}}{N_{kt}} \quad (1)$$

where  $q_{cone,t}$  is the corrected cone resistance;  $\sigma_{v0}$  is the total in-situ overburden pressure and  $N_{kt}$  is calibrated cone factor. To recognize well from ball resistance parameters, the measured and corrected cone resistances herein are termed  $q_{cone}$  and  $q_{cone,t}$ , which are normally  $q_c$  and  $q_{t}$ , respectively, in pure CPTU analyses.

### Net ball resistance and ball factor

As given in Eq. (1), the net cone resistance is obtained by subtracting the total overburden pressure ( $\sigma_{v0}$ ) from the corrected cone resistance ( $q_{cone,t}$ ). The derivation of the net ball resistance has been suggested in a similar form (Randolph, 2004):

$$q_{ball,net} = q_{ball,t} - \alpha \sigma_{v0} \quad (2)$$

where  $q_{ball,t}$  is the corrected ball resistance;  $\alpha$  is the ratio of cone cross-sectional area ( $A_{cone}$ ) to the ball projected area ( $A_{ball}$ ). The formula returns to the common expression when the ball diameter is equal to the cone diameter (i.e.,  $\alpha = 1$ ). The corrected ball resistance is obtained similarly as it is done for the cone:

$$q_{ball,t} = q_{ball} + (1 - a)u_2\alpha \quad (3)$$

where  $q_{ball}$  is measured ball resistance;  $a$  is the cone area ratio (Lunne et al. 1997); and  $u_2$  is the induced pore water pressure from the filter at the cone shoulder. If the  $u_2$  measurement is not available then the static pore water pressure ( $u_0$ ) can approximately be used (Randolph, 2004). Finally, the net ball resistance can be rearranged in more detail as follows:

$$q_{ball,net} = q_{ball} - [\sigma_{v0} - (1 - a)u_2] \frac{A_{cone}}{A_{ball}} \quad (4)$$

The ball factor is then obtained as:

$$N_{ball} = \frac{q_{ball,net}}{S_u} \quad (5)$$

where  $S_u$  is the reference undrained shear strength and it is obtained by the FVT in this study.

### Remolded ball factor

Similar to the ball factor, the remolded ball factor is defined as the ratio of the measured remolded ball resistance to the reference remolded shear strength:

$$N_{ball,rem} = \frac{q_{ball,rem}}{S_{u,rem}} \quad (6)$$

The remolded ball resistance ( $q_{ball,rem}$ ) is defined as the constant resistance value reached after a number of cyclic penetrations. The reference remolded shear strength can be obtained from lab tests (e.g., fall cone, miniature vane shear, and triaxial testing) or from field tests (e.g., FVT, CPTU). In this study, this value is obtained from the FVT.

### Undrained shear strength from the FVT

In this study, the reference undrained shear strength is taken from the FVT. The field value  $S_{u,FV}$  is corrected for strain rate and anisotropic effects (Aas et al., 1986):

$$S_{u,FV,corr} = \mu S_{u,FV} \quad (7)$$

where  $\mu$  is correction factor and it is a function of measured shear strength to the in-situ effective pressure ( $S_{u,FV}/\sigma'_{v0}$ ).

**Sensitivity**

The sensitivity of clay is theoretically defined as the ratio of the intact undrained shear strength to the remolded undrained shear strength ( $S_u/S_{u,rem}$ ). The reference sensitivity herein is obtained from the FVT and is defined as:

$$S_t = \frac{S_{u\ FV,corr}}{S_{u\ FV,rem}} \tag{8}$$

Generally, the ratio of initial penetration resistance to the remolded penetration resistance ( $q_{ball,ini}/q_{ball,rem}$ ) is not equal to the sensitivity of the soil. It is expected here to find a correlation between the sensitivity and this resistance ratio.

**TEST RESULTS AND DISCUSSIONS**

This section describes a comparison of measured, net ball and cone resistances obtained from different ball and cone sizes. The ball factors and remolded ball factors are then derived from net ball resistances. Finally, the sensitivity of the clay is examined from the cyclic penetration test.

**Measured cone and ball resistances**

Figures 5a, 5b, 5c, and 5d show the measured ball penetration and extraction resistances and induced pore water pressure profiles from the balls Type-1 to Type-4, respectively. As shown in the figures, the extraction resistances are negative (except from Type-4), which imply that soil flowed upward and occupied the space above the ball during penetration and consequently resulted in a negative resistance when the ball is extracted upward. The magnitude of the negative resistance becomes smaller with smaller ball diameter, and especially the resistance is almost zero for the ball Type-4 ( $\alpha = 1$ ).

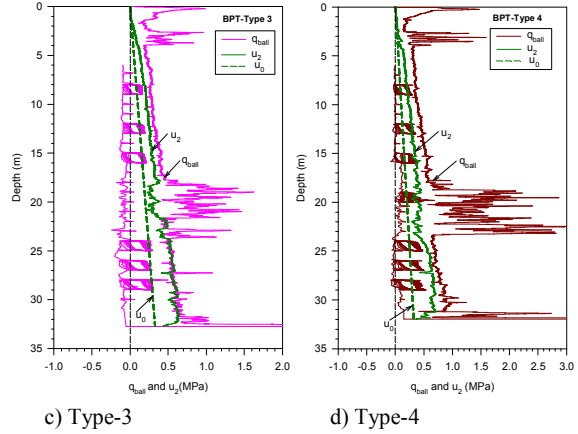
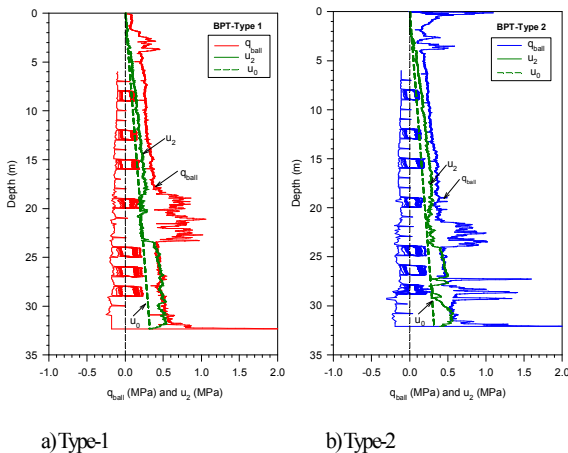


Figure 5 Measured ball resistance and pore pressure from BPT

Figure 6 shows a comparison of measured ball and cone resistances obtained from different ball and cone types, and Figure 7 shows a comparison of corresponding induced pore water pressure ( $u_2$ ). It is interesting to note from Figure 6 that the measured resistance from smaller ball (cone) diameter, in general, is larger than that from larger ball (cone) diameter, respectively. Similarly, the pore water pressure (Figure 7) induced from smaller ball (cone) diameter is larger than that from the larger ball (cone) diameter, respectively.

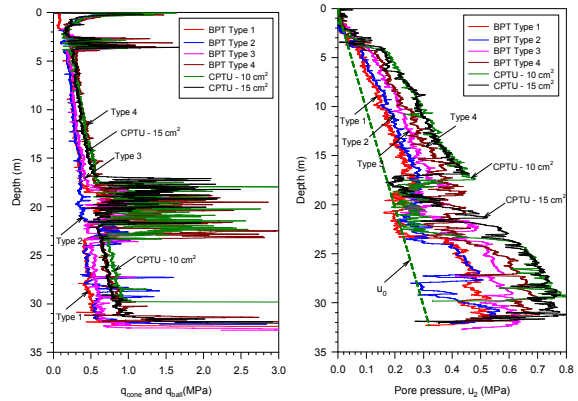


Figure 6 (left) Comparison of measured cone and ball penetration resistances ( $q_{ball}$  and  $q_{cone}$ ). Figure 7 (right) Comparison of induced pore water pressure ( $u_2$ )

For cone penetration test, the finding of larger measured cone resistance resulted from smaller cone diameter herein agrees well with similar findings from De Lima and Tumay (1991) [with cones of 1.27 cm<sup>2</sup>, 10 cm<sup>2</sup>, and 15 cm<sup>2</sup>] and Titi et al. (2000) [with cones of 2 cm<sup>2</sup> and 15 cm<sup>2</sup>]. The main reasons that cause the difference are (Lunne et al. 1997): (i) the difference of pore water pressure field around the cone in soft clayey soils (especially for cones with different area ratios,  $a$ ); (ii) in layered soil profiles, the larger cone penetrometer needs a

thicker layer to reach a steady cone resistance. Therefore, in several layers smaller cone may reach a “plateau” of cone resistance while this may not be so with the larger diameter cone.

For ball penetrometer, besides the two possible reasons mentioned above, another main reason is probably that larger ball diameter (with the use of the same cone probe) makes larger space behind the ball that allows soil to flow upward and leads to a significant release of compressive stress right beneath the ball.

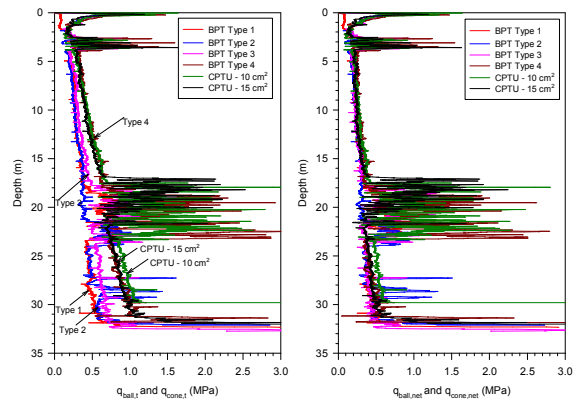


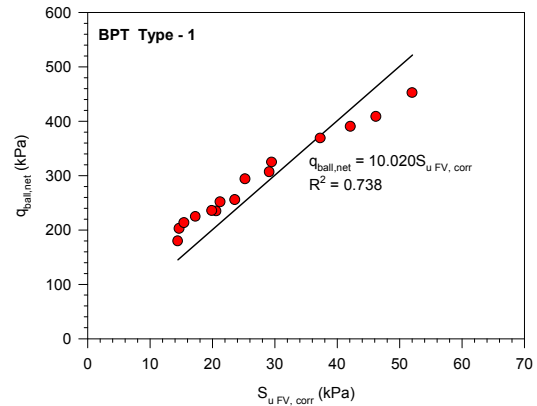
Figure 8 (left) Comparison of corrected cone and ball resistances ( $q_{ball,corr}$  and  $q_{cone,corr}$ ). Figure 9 (right) Comparison of net ball and cone resistances ( $q_{ball,net}$  and  $q_{cone,net}$ ).

Figure 8 shows a comparison of corrected ball and cone resistances [Eq. (3)]. It is noted that the corrected resistances show the same trend to that from the measured ball and cone resistances (Figure 6). However, it is very interesting to learn that the net ball and cone resistances are very similar results, as shown in Figure 9, except the lower part of CPTU-10 cm<sup>2</sup> profile. The similarity of net ball resistances profile suggests that any ball diameters would yield similar ball factors (thus the undrained shear strengths).

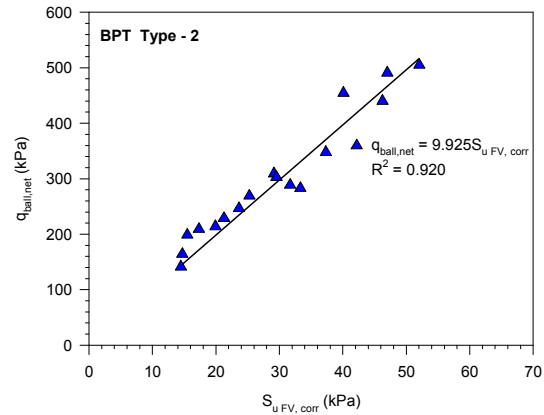
### Ball and cone factors

It is well known that the undrained shear strength ( $S_u$ ) is not a fundamental soil parameter but its value depends on the mode of shearing, strength anisotropy, strain rate and stress history. In addition,  $S_u$  also depends on the quality of the sample that is sheared. Besides the general dependences above, the cone factor (e.g.,  $N_{kt}$ ), and therefore  $S_u$  derived from this cone factor, particularly depends on: rigidity index ( $I_r = G/S_u$  where  $G$  is the soil shear modulus); the normalized in-situ stress difference between vertical ( $\sigma_{v0}$ ) and horizontal ( $\sigma_{h0}$ ) stresses ( $\Delta = (\sigma_{v0} - \sigma_{h0})/2S_u$ ); interface friction coefficient ( $\alpha_i = 0$  to 1); and strength anisotropy ratio ( $\rho = S_{ue}/S_{uc}$ ) (Teh and Houlsby, 1991; Lu et al., 2004; Su and Liao, 2002).

Among these factors, the rigidity index plays a vital role in the variation of the cone factor.



a) Type-1

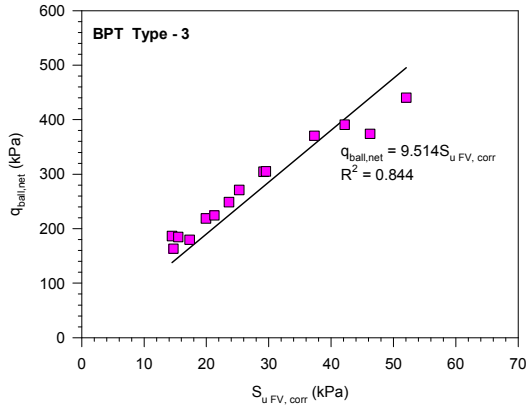


b) Type-2

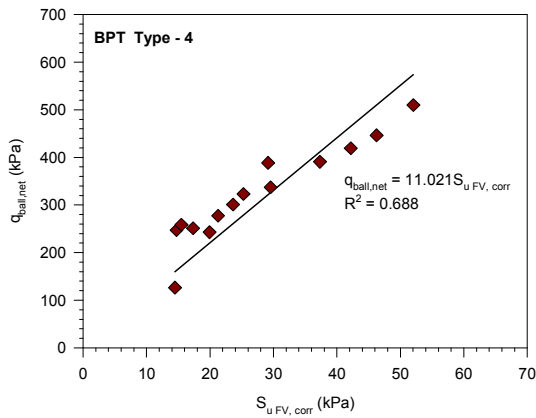
Figure 10 Correlation between  $q_{ball,net}$  and  $S_{u,FV,corr}$

Figures 10a, 10b, 10c, and 10d show the correlation between  $q_{ball,net}$  and  $S_{u,FV,corr}$  for balls Type-1 to Type-4, respectively, after removing some extremely non-banded data points resulted from the dense shell intercalated layer. As anticipated from the similar net resistances (Figure 9), the ball factors ( $N_{ball}$ ) are quite similar (except the value from ball Type-4), changing from 10.026 (Type-1) to 9.514 (Type-3).

These similar ball factors with relatively high values of coefficient of determination ( $R^2$ ) indicate that the ball size, herein  $\beta = 0.15$  to 0.50, is not a key factor controlling the magnitude of the ball factor if the in-situ overburden pressure ( $\sigma_{v0}$ ) and undrained shear strength ( $S_u$ ) are properly evaluated. Similar finding was also reported by Nakamura et al. (2009) for 3 ball sizes of  $\beta = 0.1, 0.3,$  and  $0.6$ . The ball Type-4 is actually a modified form of the conventional cone, and the ball factor is slightly larger than the values from the other balls.

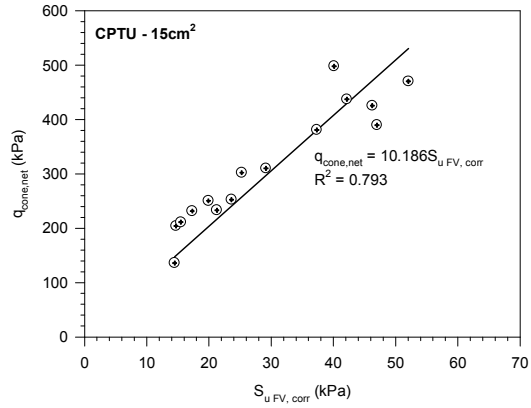


c) Type-3

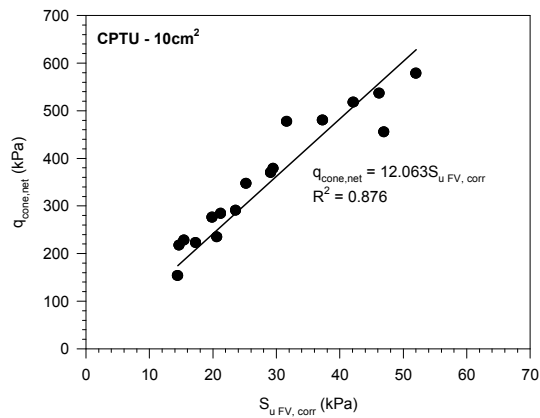


d) Type-4

Figure 10 (cont.) Correlation between  $q_{ball,net}$  and  $S_{u FV,corr}$



a) Cone 15 cm<sup>2</sup>



b) Cone 10 cm<sup>2</sup>

Figure 11 Correlation between  $q_{cone,net}$  and  $S_{u FV,corr}$

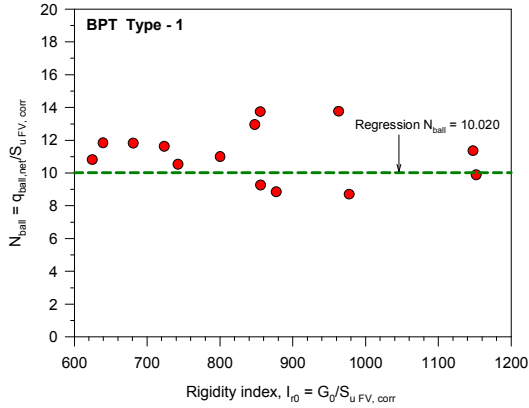
Similarly, Figures 11a and 11b show the relationship between the net cone resistance  $q_{net,cone}$  and  $S_{u FV,corr}$  for the cone types of 15 cm<sup>2</sup> and 10 cm<sup>2</sup>, respectively. As a result, the cone factor resulted from the cone of 15 cm<sup>2</sup> ( $N_{kt} = 10.186$ ) is quite similar to the ball factors since the net cone resistances are almost the same as the net ball resistances (Figure 9). The cone factor resulted from the cone of 10 cm<sup>2</sup> is slightly higher ( $N_{kt} = 12.063$ ) due to the higher values of net cone resistances in the lower clay layer (Figure 9).

As discussed above, the cone factor depends largely on the rigidity index ( $I_r = G/S_u$ ), which differs from site to site, even from layer to layer at the same site. Thus, the current practice of estimating  $S_u$  from the CPTU still relies heavily on empirical and local correlations. Figures 12a, 12b, 12c, and 12d show the relationship between ball factor ( $N_{ball}$ ) and the maximum rigidity index ( $I_{r0}$ ) defined as the ratio of maximum shear modulus ( $G_0$ ) to the reference undrained shear strength ( $S_{u FV,corr}$ ). The maximum shear modulus was obtained from the SDMT at every 0.5m intervals at the site.

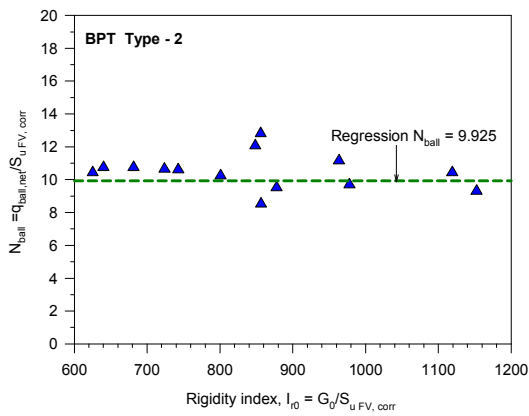
It is shown from the figures that the ball factors obtained ball Type-1, Type-2, and Type-3 are independent of the rigidity index. The data points are slightly scattered due to the mismatch of cross-correlations between the BPT, SDMT, and FVT. As shown in Figure 12d, with exception of the scattered data points, the ball Type-4 produced a clear trend that the ball factor increases with increasing of the rigidity index.

Similar results were found from the cones of 15 cm<sup>2</sup> and 10 cm<sup>2</sup> as shown in Figures 13a and 13b, respectively. The independence of ball factor on the rigidity index was also found and reported by Lu et al. (2000); Low (2009). The dependence of the cone factor on the rigidity, as shown in this study, has already clearly stated in the literature (Teh and Houlsby, 1991; Lu et al., 2004; Su and Liao, 2002).

The dependence of the cone factor on the rigidity index implies that it can only be applied to the particular site (or even layer) where the factor was derived. At other sites, where the stress history and geological depositional environment are different, the factor is not reliable.



a) Type-1



b) Type-2

Figure 12 Correlation between  $N_{ball}$  and  $I_{r0}$

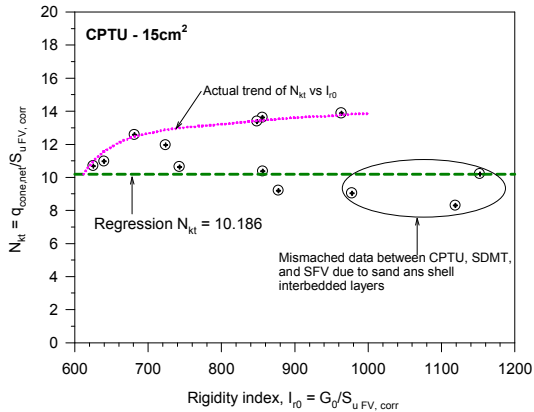
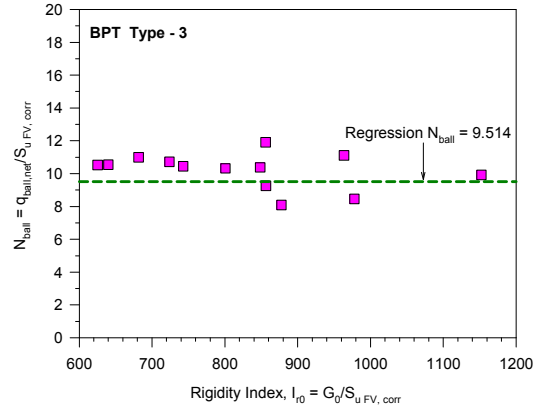
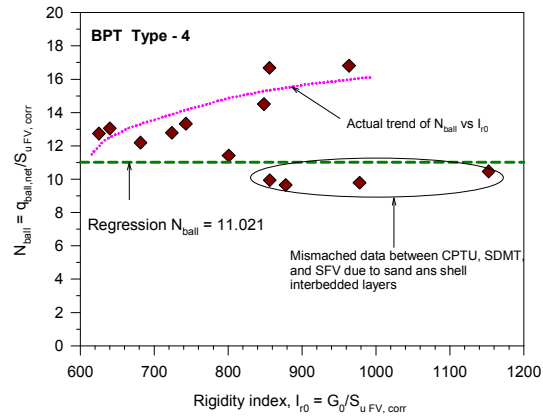


Figure 13a Correlation between  $N_{kt}$  and  $I_{r0}$ : cone 15 cm<sup>2</sup>

Figure 14 shows a comparison of regression ball and cone factors obtained from this study and the theoretical upper and lower bound values proposed by Randolph (2000, 2004) for the BPT. The theoretical values were obtained from plasticity solutions applied to homogeneous, perfectly plastic materials with considering the ball roughness effect. Figure 14 shows two values obtained from the ball of 113 mm in diameter.



c) Type-3



d) Type-4

Figure 12 (cont.) Correlation between  $N_{ball}$  and  $I_{r0}$

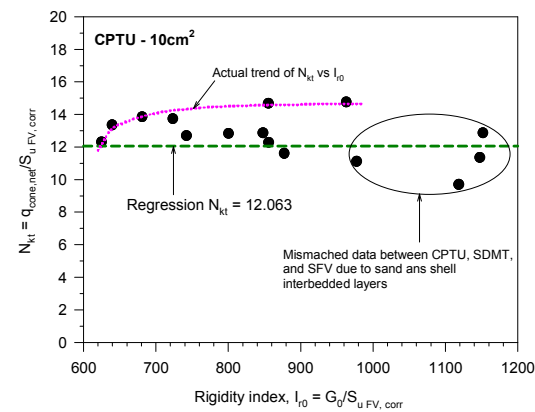


Figure 13b Correlation between  $N_{kt}$  and  $I_{r0}$ : cone 10 cm<sup>2</sup>

(in association with cone diameter of 10 cm<sup>2</sup>) and a recommended practice value for interface friction coefficient of  $\alpha_s = 0.3$ .

The figure shows that the ball factors obtained from this study are slightly smaller than those from the theoretical solutions. The discrepancy probably comes the actual soil conditions (e.g., soil heterogeneity, non-perfectly plastic

material) which are different from idealized ones. The average value ball factor herein obtained from balls Type-1 to Type-3 is approximately 10.0. It is not sufficient to conclude the best ball type from this study since the test was carried out at only one study site resulting in similar regression ball factors and relatively high values of coefficient of determination. Theoretically, the best ball type is the one which minimizes the uncertainty of estimated in-situ overburden pressure and produce the best resolution profile (i.e., ball Type -1).

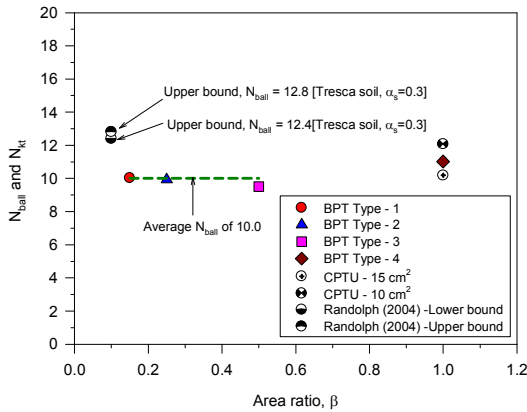


Figure 14 Comparison of ball and cone factors

### Resistance degradation

The strength lost during cyclic penetration test indicates the strain softening behavior of the test soil. Generally, the higher sensitivity the soil possesses, the larger degree of resistance degradation the soil exposes. Figure 15 shows a typical test point of cyclic penetrations from ball Type-1. It was observed from the field that the penetration resistance at the 8<sup>th</sup> cycle was almost constant, thus the cyclic test was completed at the 8<sup>th</sup> cycle for all test points and ball types.

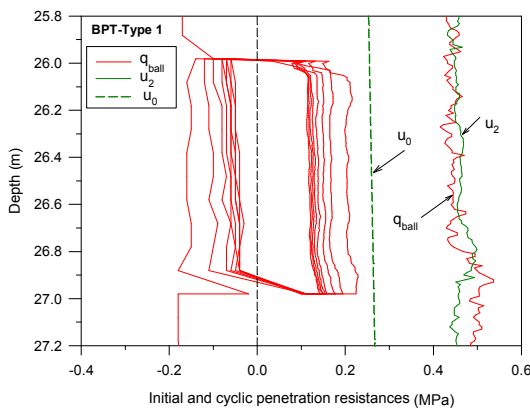
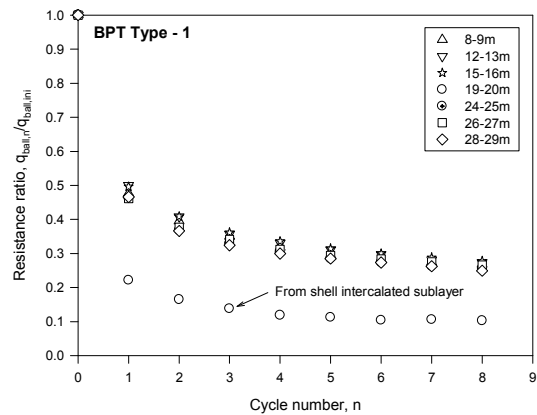


Figure 15 A typical cyclic penetration test from ball Type-1

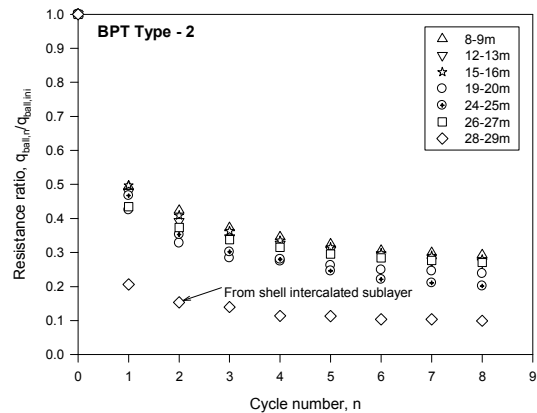
Figures 16a, 16b, 16c and 16d show cyclic resistance ratios of penetration resistance at cycle  $n^{th}$  ( $q_{ball,n}$ ) to the initial penetration resistance ( $q_{ball,ini}$ ) versus the cycle number ( $n$ ) obtained from ball Type-1 to Type-4, respectively. It is shown from the figures that the remolded ball resistance ( $q_{ball,rem}$ ) was not completely reached, however the further decrease of resistance would be insignificant if more number of cycles were performed.

The ball Type-4 produced some abnormal curves which reached the smallest resistance ratio and again increased before gradually approaching the remolded state. This behavior was resulted from the fact that small ball like Type-4 is very sensitive to the heterogeneity of soil. The influence of the heterogeneity decreases with increasing of ball diameter. Especially, the biggest ball (Type-1) produced very similar resistance ratios at different depths (except the test depth in shell intercalated sub-layer).

It is observed from the figures that the smaller ball reached to the remolded state earlier than the bigger one. This behavior is attributed to the quantity of soil brought to the remolded state. The bigger ball compresses

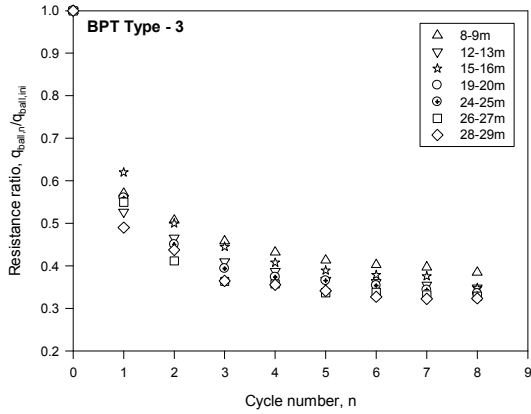


a) Type-1

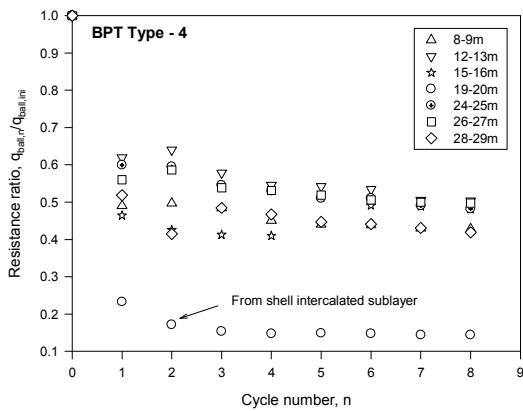


b) Type-2

Figure 16 Degradation of cyclic ball penetration resistances



c) Type-3



d) Type-4

Figure 16 (cont.) Degradation of cyclic ball penetration resistances

a larger area and takes more soil flowing backward the ball, consequently, at the same speed and number of cycles, the larger amount of soil takes more time to be remolded. It is also noted that the smaller ball reached to the remolded state with larger ratio of  $q_{ball,n}/q_{ball,ini}$  than the bigger one. This behavior can clearly be observed in Figure 17 in which the ratios were typically plotted from the same test depth.

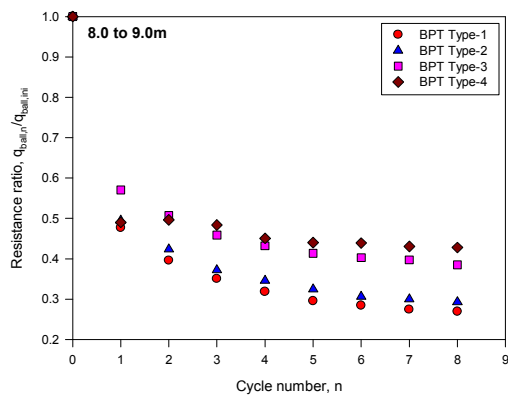
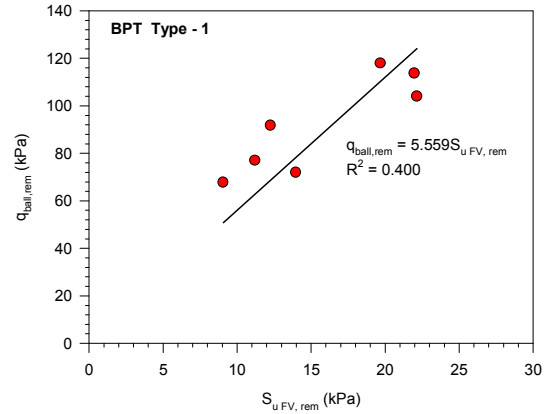
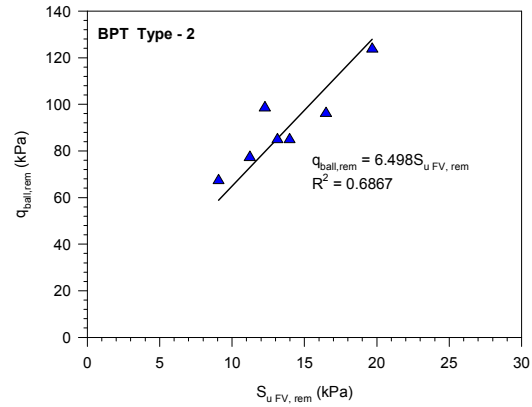


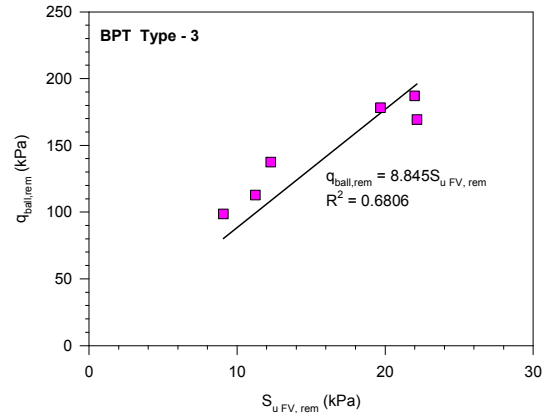
Figure 17 Magnitude of ratio  $q_{ball,n}/q_{ball,ini}$  versus ball types



a) Type-1



b) Type-2



c) Type-3

Figure 18 Remolded ball factors from three balls

### Remolded ball factor

Figures 18a, 18b and 18c show the correlation between the remolded ball resistance ( $q_{ball,rem}$ , taken at the 8<sup>th</sup> cycle) and the remolded undrained shear strength from the FVT ( $S_{u,FV,rem}$ ) for ball Type-1 to Type-3, respectively. Due to a few available data points the distribution is rather scattered with relatively low coefficient of

determination, however the correlation trend is clearly exposed. As can be anticipated from the behavior shown in Figure 17, smaller ball produced larger remolded ball factor with  $N_{ball,rem} = 8.845, 6.498$  and  $5.559$  for ball Type-3, Type-2 and Type-1, respectively. It is clearly indicated from these factors that the remolded ball resistance of the same soil depends very much on ball size.

The remolded ball factor obtained from ball Type-1 herein is rather smaller than the values of  $N_{ball,rem} = 13.6$  to  $21.7$  reported by Yafrate et al. (2009) who used the same ball diameter ( $D_{ball} = 113$  mm) to carry out cyclic penetration tests in Amherst (the U.S.), Burswood (Australia), Gloucester (Canada), and Onsoy (Norway). The reason of higher remolded ball factors from Yafrate et al.'s analysis is that the tests were carried out in higher sensitive soils (Amherst  $S_t = 7.3$ ; Burswood:  $S_t = 3.9$ ; Gloucester:  $S_t = 68$ ; Onsoy:  $S_t = 6.0$ ) than clay in this study (average  $S_t = 2.2$ ).

### Sensitivity

The sensitivity values obtained from the FVT at the test site are plotted against the ratios of initial ball penetration resistance ( $q_{ball,ini}$ ) to the remolded ball penetration resistance ( $q_{ball,rem}$ ) as shown in Figure 19. It is shown that no good correlation can be made between the sensitivity values and the resistance ratios from any ball types since the test was carried out at only one site having rather constant sensitivity. It is only possible to conclude from this study site that the sensitivity is smaller than the resistance ratio of  $q_{ball,ini}/q_{ball,rem}$ . In contrast, Yafrate et al. (2009) proposed a correlation from higher sensitive soils as plotted in the figure.

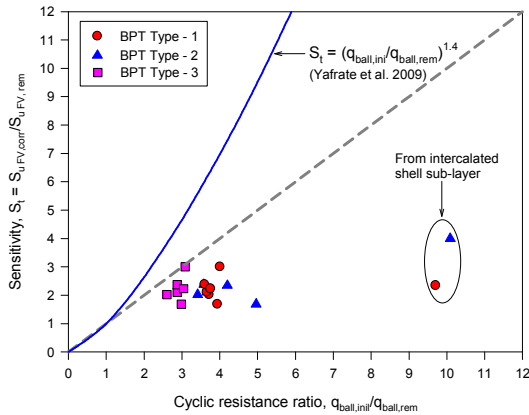


Figure 19 Sensitivity versus ratio of  $q_{ball,ini}/q_{ball,rem}$

### CONCLUSIONS

The ball penetration test (BPT) was carried out at an investigation site in the Nakdong River delta, Busan, S. Korea. To examine the effect of ball sizes to the penetration resistance and ball factor, the test was carried

out by using four different ball sizes having area ratios of 0.15 (Type-1), 0.25 (Type-2), 0.5 (Type-3) and 1.0 (Type-4). For each ball type, cyclic test (penetrations and extractions) of 8 cycles was carried out at several depths to evaluate the remolded penetration resistance and consequently the sensitivity of the clay. The cyclic length of 1.0 m was applied for all test points. To calibrate the BPT results, the CPTU with cones of  $10\text{ cm}^2$  and  $15\text{ cm}^2$ , field vane test (FVT) and seismic dilatometer test (SDMT) were also carried at the site. Both the CPTU and BPT were carried out at the same speed of  $20\text{ mm/s}$ . The following conclusions can be drawn from this study:

- 1) The measured ball and cone penetration resistances ( $q_{ball,ini}$ ,  $q_{cone}$ ) are size-dependent values. Generally, smaller cone (or ball) diameter produces larger penetration resistance and larger pore water pressure ( $u_2$ ).
- 2) The net ball and cone resistances of different sizes are found very similar. This finding implies that the balls and cones would yield similar ball and cone factors ( $N_{ball}$ ,  $N_{kt}$ ) if the in-situ overburden pressure ( $\sigma_{v0}$ ) and reference undrained shear strength ( $S_u$ ) are properly evaluated.
- 3) The ball factors ( $N_{ball}$ ) obtained from balls Type-1, Type-2 and Type-3 are 10.020, 9.925, and 9.514, respectively. These similar ball factors are slightly smaller than the theoretical values proposed by Randolph (2004).
- 4) The ball factors obtained from Type-1, Type-2 and Type-3 are found independent on the rigidity index ( $I_{r0}$ ), whereas the values obtained from ball Type-4 and cones are dependent.
- 5) It is found that the ball size greatly influences the remolded ball factor. Smaller ball produced larger remolded ball factor.
- 6) Sensitivity of the test soil is smaller than the ratio of  $q_{ball,ini}/q_{ball,rem}$ , however no good correlation was obtained.

### ACKNOWLEDGEMENTS

This work was supported by the Korea Science and Engineering Foundation (KOSEF) NRL Program grant funded by the Korea government (MEST) (No. R0A-2008-000-20076-0).

### REFERENCES

- Aas, G., Lacasse, S., Lunne, T. and Hoeg, K. (1986). Use of In Situ Tests for Foundation Design on Clay. In Use of in situ tests in geotechnical engineering, *Geotechnical special publication* No. 6, 1986, ASCE, 1-30.
- Boylan, N. and Long, M. (2007). Characterisation of Peat

- Using Full-Flow Penetrometers. *Soft Soil Engineering*, Chan and Law (ed.), Taylor & Francis Group, London, 403-414.
- Chung, S.F. and Randolph, M.F. (2004). Penetration Resistance in Soft Clay for Different Shaped Penetrometers. *Proceedings of Geotechnical and Geophysical Site Characterization, ISC-2*, Viana da Fonseca and Mayne (ed.), 671-677.
- Chung, S.G., Ryu, C.K., Min, S.C., Lee, J.M. and Hong, Y.P. (2010). Geotechnical Properties and Depositional Environment of Clay in the Floodplain of the Nakdong River Delta. *KSCE Journal of Civil Engineering* (in review).
- Chung, S.G. and Kweon, H.J. (2010). Oil-operated fixed piston sampler and its applicability. *Journal of Geotechnical and Geoenvironmental Engineering*, ASCE (in review).
- De Lima, D.C. and Tumay, M.T. (1991). Scale Effects in Cone Penetration Tests. *Proceedings of the Geotechnical Congress 1991*, ASCE, Boulder, Colorado, Vol.1: 38-51.
- Einav, I. and Randolph, M.F. (2005). Combining Upper and Lower Bound and Strain Path Methods for Evaluating Penetration Resistance. *International Journal of Numerical in Engineering*, 69:1991-2016
- ISSMGE (1999). International Society of Soil Mechanics and Geotechnical Engineering. International Reference Test Procedure for Cone Penetration Test (CPT) and Cone Penetration Test with Pore Pressure (CPTU), *Proceedings of the Twelfth European Conference on Soil Mechanics and Geotechnical Engineering*, Amsterdam, Barends et al. (ed.) Vol.3: 2195-2222.
- Low, H.E., Randolph, M.F., DeJong, J.T. and Yafate, N.J. (2008). Variable Rate Full-Flow Penetration Tests in Intact and remoulded Soils, *Proceedings of Geotechnical and Geophysical Site Characterization*, Hwang and Mayne (ed.), Taylor & Francis Group, London, 1087-1092.
- Low, H.E. (2009). Performance of Penetrometers in Deepwater Soft Soil Characterization, *PhD Thesis*, The University of Western Australia, Australia.
- Lu, Q., Hu, Y. and Randolph, M.F. (2000). FE Analysis for T-bar and Spherical Penetrometers in Cohesive Soils. *ISOPE 2000*, Seattle, Vo. 2, 617-623.
- Lu, Q. Randolph, M.F., Hu, Y. and Bugarski, I.C. (2004). A Numerical study of Cone Penetration Test in Clay. *Geotechnique*, 54(4), 257-267.
- Lunne, T., Robertson, P.K. and Powell, J.J.M. (1997). Cone Penetration Testing in Geotechnical Practice, 1st edition, 1997. *Blackie Academic & Professional*, London, UK.
- Mayne, P.W. (2007). Cone Penetration Testing. *National Cooperative Highway Research Program*, NCHRP Synthesis 386.
- Nakamura, A., Tanaka, H. and Fukasawa, T. (2009). Application of T-bar and Ball Penetration Tests to Soft Clayey Grounds. *Soils and Foundations*, 49(5):729-738.
- Randolph, M.F. Martin, C.M. and Hu, Y. (2000). Limiting Resistance of A Spherical Penetrometer in Cohesive Material. *Geotechnique*, 50(5):573-582.
- Stewart, D.P. and Randolph, M.F. (1991). A New Site Investigation Tool for the Centrifuge. *Proceeding of International Conference on Centrifuge*, H.Y. Ko (ed.), Balkema, 531-538.
- Stewart, D.P. and Randolph, M.F. (1994). T-bar Penetration Testing in Soft Clay. *Journal of Geotechnical Engineering*, ASCE 120(12): 2230-2235.
- Su, S.F. and Liao, H.J. (2002). Influence of Strength Anisotropy on Piezocon Resistance in Clay. *Journal of Geotechnical and Geoenvironmental Engineering*, 128(2): 166-173.
- Teh, C.I. and Houlsby, G.T. (1991). An Analytical Study of the Cone Penetration Test in Clay. *Geotechnique*, 41(1):17-34.
- Titi, H.H., Mohammad, L.N. and Tumay, M.T. (2000). Miniature Cone Penetration Tests in Soft and Stiff Clays. *Geotechnical Testing Journal*, 23(4): 432-443
- Vallejo, L.E. (1982). Evaluation of Test Methods Designed to Obtain the Undrained Shear Strength of Muds. *Proceedings of 14th Annual Offshore Technology Conference*, Paper OTC 4320.
- Yafate, N., DeJong, J., Degroot, D. and Randolph, M.F. (2009). Evaluation of Remolded Shear Strength and Sensitivity of Soft Clay Using Full-Flow Penetrometers. *Journal of Geotechnical and Geoenvironmental Engineering*, ASCE, 135(9):1179-1189.
- Zhou, H. and Randolph, M.F. (2009). Resistance of Full-Flow Penetrometers in Rate-dependent and Strain-Softening Clay. *Geotechnique*, 59(2):79-86.